The Superior Frontal Transsulcal Approach to the Anterior Ventricular System: Exploring the Sulcal and Subcortical Anatomy Using Anatomic Dissections and Diffusion Tensor Imaging Tractography

Christos Koutsarnakis[1,3], Faidon Liakos[1], Aristotelis V. Kalyvas[1,2], Georgios P. Skandalakis[1,6], Spyros Komaitis[1,2], Fotini Christidi[4], Efstratios Karavasilis[5], Evangelia Liouta[7], George Stranjalis[1,2]

■ OBJECTIVE: **To explore the superior frontal sulcus (SFS) morphology, trajectory of the applied surgical corridor, and white matter bundles that are traversed during the superior frontal transsulcal transventricular approach.**

■ METHODS: **Twenty normal, adult, formalin-fixed cerebral hemispheres and 2 cadaveric heads were included in the study. The topography, morphology, and dimensions of the SFS were recorded in all specimens. Fourteen hemispheres were investigated through the fiber dissection technique whereas the remaining 6 were explored using coronal cuts. The cadaveric heads were used to perform the superior frontal transsulcal transventricular approach. In addition, 2 healthy volunteers underwent diffusion tensor imaging and tractography reconstruction studies.**

■ RESULTS: **The SFS was interrupted in 40% of the specimens studied and was always parallel to the interhemispheric fissure. The proximal 5 cm of the SFS (starting from the SFS precentral sulcus meeting point) were found to overlie the anterior ventricular system in all hemispheres. Five discrete white matter layers were identified en route to the anterior ventricular system (i.e., the arcuate fibers, the frontal aslant tract, the external capsule, internal capsule, and the callosal radiations). Diffusion tensor imaging studies confirmed the fiber tract architecture.**

■ CONCLUSIONS: **When feasible, the superior frontal transsulcal transventricular approach offers a safe and effective corridor to the anterior part of the lateral ventricle because it minimizes brain retraction and transgression and offers a wide and straightforward working corridor. Meticulous preoperative planning coupled with a sound microneurosurgical technique are prerequisites to perform the approach successfully.**

INTRODUCTION

Surgery of the anterior part of the ventricle remains a distinct challenge in neurosurgery because of its complex regional neurovascular anatomy[1-5] and because there is still controversy surrounding the most versatile operative corridor for each case. Traditionally, the 2 most commonly used surgical approaches have been the transcortical and transcallosal pathways, both of which offer direct and effective access with what was previously believed to be minimal brain transgression.[6-14]

However, the microneurosurgical concept of using normal cerebral corridors, such as fissures, cisterns, and sulci, to resect deep-seated lesions[15-21] has led to the evolution of a theoretically more delicate approach to the anterior part of the lateral ventricle and foramen of Monro through the superior frontal sulcus (SFS), known as the superior frontal transsulcal

Key words
- DTI
- Frontal lobe
- Transsulcal approaches
- Ventricular surgery
- White matter anatomy

Abbreviations and Acronyms
DTI: Diffusion tensor imaging
FAT: Frontal aslant tract
MRI: Magnetic resonance imaging
ROI: Region of interest
SFS: Superior frontal sulcus
SLF: Superior longitudinal fasciculus

From the [1]Athens Microneurosurgery Laboratory and [2]Department of Neurosurgery, Evangelismos Hospital, Athens, Greece; [3]Department of Clinical Neuroscience, Western General Hospital, Edinburgh, United Kingdom; [4]2nd Department of Radiology, School of Medicine, University of Athens, Athens, Greece; [5]Department of Neurology, Aeginition Hospital, University of Athens, Athens, Greece; [6]School of Medicine, University of Athens, Athens, Greece; and [7]Hellenic Center for Neurosurgical Research, "Petros Kokkalis", Athens, Greece

To whom correspondence should be addressed: Christos Koutsarnakis, M.D. [E-mail: ckouts@hotmail.co.uk]

Christos Koutsarnakis, Faidon Liakos, and Aristotelis V. Kalyvas contributed equally to this study.

Citation: World Neurosurg. (2017) 106:339-354.
http://dx.doi.org/10.1016/j.wneu.2017.06.161

Journal homepage: www.WORLDNEUROSURGERY.org

Available online: www.sciencedirect.com

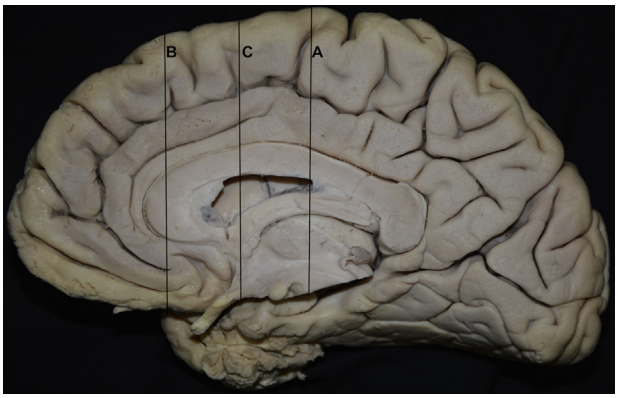

Figure 1. The medial surface of a left hemisphere. The black lines represent the levels of coronal cuts made. *A*, level of the intersection point of the precentral—superior frontal sulcus; *B*, level of the genu of the corpus callosum; *C*, middle of the distance between the 2 aforementioned levels.

transventricular approach.[16,22] During this approach, meticulous sulcal dissection is performed to minimize normal brain violation and permit optimal access to the ventricles. This ventricular operative variant has become more popular particularly because of the incorporation of sophisticated neuroimaging into everyday neurosurgical practice.

Neurosurgeons seem to have a gross and rather vague understanding of the lateral frontal lobe anatomy both in terms of surface morphology and underlying white matter architecture. More specifically and in the context of the superior transsulcal transventricular approach, data about the accurate topography and internal configuration of the SFS along with detailed knowledge of the fiber pathways transgressed during the approach are lacking in the neurosurgical literature. Hence, our main objective was to shed light on these issues by exploring the relevant anatomy both in cadaveric specimens through laboratory dissections and in normal individuals by using diffusion tensor imaging (DTI) studies.

To our knowledge, this is the first anatomic and imaging description of the superior frontal transsulcal approach aiming to provide a thorough three-dimensional understanding of the regional cortical and subcortical architecture for surgical practice.

METHODS

The study was divided into 2 parts and included laboratory cadaveric dissections and DTI imaging in normal individuals.

In the first part of the study, we used 20 normal, adult, cadaveric cerebral hemispheres (12 right hemispheres, 8 left hemispheres) obtained from 20 different cadavers, previously fixed in a 10%–15% formalin solution for a minimum period of 2 months. Arachnoid membrane and vessels were carefully removed and the topography, morphology, and dimensions of the SFS were thoroughly studied and recorded in all specimens. The SFS was defined as the sulcus demarcating the superior from the middle frontal gyrus, originating adjacent (posterior, anterior, or coincident) to the precentral sulcus and terminating close to the frontal pole.[23,24] The presence of a medial and/or middle frontal sulcus, which can add uncertainty to the proper identification of the SFS, was also recorded and their respective distance from the interhemispheric fissure was measured to clarify the surface anatomy of the lateral frontal lobe.

Fourteen hemispheres underwent the Klingler procedure and were explored through the fiber microdissection technique. The aim was to investigate and show the white matter pathways lying in or adjacent to the surgical corridor applied during the superior transsulcal transventricular approach. Ten specimens were dissected in a lateromedial direction,[25,26] 2 specimens were dissected in a mediolateral direction so as to show the anterior callosal fibers more accurately, and the remaining 2 hemispheres were explored both in a lateromedial and mediolateral direction to show the intermingling fibers of the corpus callosum and internal capsule at the level of the SFS.

Six specimens were investigated through coronal cuts made at 3 different levels along the length of the sulcus (**Figure 1**). The first cut was placed at the level of the SFS—precentral sulcus meeting point. The second cut was made at the level of the genu of the corpus callosum, which demarcates the anterior limit of the lateral ventricle, and the third cut was made in the middle between the 2 previous cuts. The rationale was to isolate and

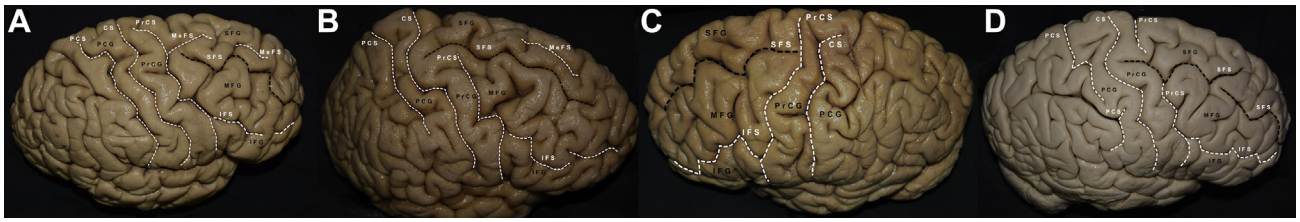

Figure 2. Three different hemispheres showing the morphologic variability of the superior frontal sulcus (SFS) and regional surface anatomy of the superolateral frontal lobe. (**A**) A right cerebral hemisphere showing an interrupted SFS with its originating point anterior to the precentral sulcus. An interrupted medial frontal sulcus is also apparent. (**B**) In this specimen, the SFS has a continuous pattern and its originating point lies posterior to the precentral sulcus. Note the presence of a prominent interrupted medial frontal sulcus. (**C**) A left hemisphere showing a continuous SFS with its originating point coincident to the precentral sulcus. (**D**) A right hemisphere with an interrupted SFS and its originating point posterior to the precentral sulcus. CS, central sulcus; IFG, inferior frontal gyrus; IFS, inferior frontal sulcus; MeFS, medial frontal sulcus; MFG, middle frontal gyrus; PCG, postcentral gyrus; PCS, postcentral sulcus; PrCG, precentral gyrus; PrCS, precentral sulcus; SFG, superior frontal gyrus.

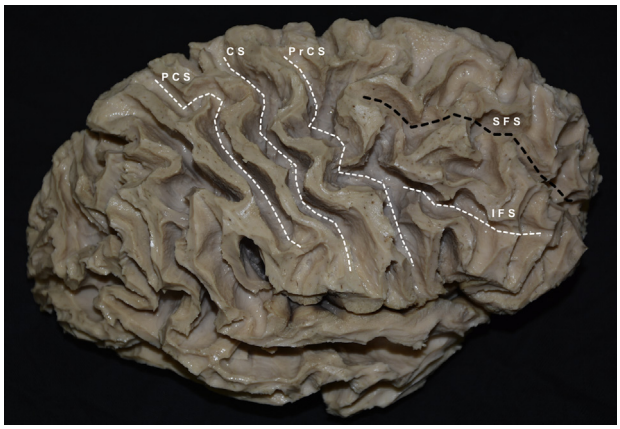

Figure 3. The arcuate fibers after peeling of the gray matter of the specimen in Figure 2A are shown. Dotted lines represent the sulci of the frontal and central areas. CS, central sulcus; IFS, inferior frontal sulcus; PCS, postcentral sulcus; PrCS, precentral sulcus; SFS, superior frontal sulcus.

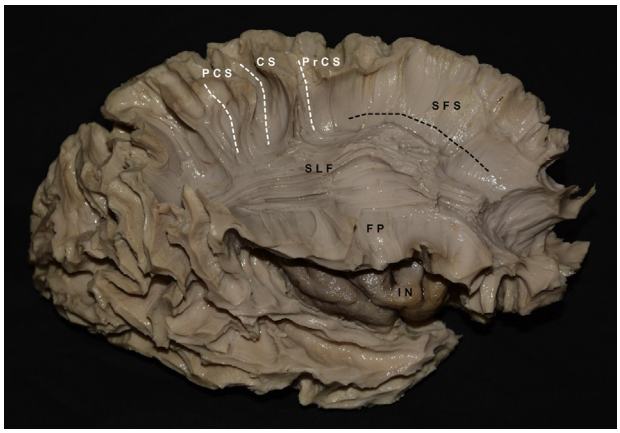

Figure 4. The same specimen, after dissection of the arcuate fibers. The horizontal segment of the superior longitudinal fasciculus (SLF) is exposed. The superior longitudinal fasciculus was always seen to run inferior to the level of the superior frontal sulcus (SFS) and more specifically at the level of the middle frontal gyrus. The dotted black line represents the level of the superior frontal sulcus. The insular cortical surface is also apparent. CS, central sulcus; FP, frontoparietal operculum; IN, insula; PCS, postcentral sulcus; PrCS, precentral sulcus.

measure the segment of the sulcus that corresponds to the deep-seated lateral ventricle and to investigate the relevant anatomic correlations. The respective distance between the fundus of the sulcus and the lateral ventricle was subsequently measured and recorded for every cut made.

In addition, 2 formalin-fixed normal adult cadaveric heads were used to perform and demonstrate the superior frontal transsulcal approach to the anterior part of the ventricular system. Skin incision, tailoring of the craniotomy, identification of the SFS, and opening of the arachnoid covering along its exposed length, placement of brain spatulas, and subsequent subcortical dissection en route to the ventricle are shown for educational purposes before the clinical application of the approach.

Photographs were taken from every stage of all cadaveric dissections. None of the figures included has been edited by photo-enhancing software and thus, they closely resemble the anatomy encountered during the dissection process.

For the second part of the study, 2 healthy participants (30 and 31 years old) were enrolled. Both individuals underwent brain imaging in a 3-Tesla magnetic resonance imaging (MRI) scanner (Achieva TX [Philips, Best, The Netherlands]) with an 8-channel SENSE head coil. Anatomic imaging was performed with axial three-dimensional T1-weighted and T2 fluid-attenuated inversion recovery acquisitions. DTI parameters included axial single-shot spin-echo echo-planar imaging sequence with 30 diffusion encoding directions; field of view, 256 mm; acquisition voxel size, $2 \times 2 \times 2$ mm^3; repetition time, 7299 milliseconds; echo time, 68 milliseconds; flip angle, 90°; sensitivity encoding reduction factor, 2; 2 b factors with 0 seconds/mm^2 (low b) and 1000 seconds/mm^2 (high b) with 2 b factors averaged per b value, to ensure better signal-to-noise ratio. The acquisition consisted of 70 slices. DTI images were processed by the FiberTrak package (Philips, Best, The Netherlands). Before DTI analysis, diffusion registration was performed to correct for movement of the participant and susceptibility-induced distortions. DTI tractography was based on the FACT (Fiber Assignment with Continuous Tracking) algorithm.

We applied both the single and multiple region of interest (ROI) approach based on anatomic landmarks derived from the fiber dissection technique or previously used tractography protocols. We initially identified the fibers passing through a single ROI placed on a coronal plane at a level at which the SFS was clearly demarcated. A narrow oval ROI included the white matter interposed between the SFS and the anterior lateral ventricle. All tracts passing through this ROI with a minimum functional anisotropy of 0.11 and maximum angle change of 27° were traced. Moreover, to investigate the topographic relationship of the subcomponents of the superior longitudinal fasciculus (SLF; SLF I, SLF II, SLF III, arcuate fasciculus) at the aforementioned brain area, a multiple ROI approach was used according to previous described protocols for anatomic landmarks and DTI threshold parameters.[27]

We included 2 different axial MRI cuts with their respective three-dimensional volume renderings (acquired using the OsiriX application) so as to show the process of mapping the morphology of the SFS and the superolateral frontal lobe. Informed consent was obtained from every individual before the inclusion of scans and photographs in this study.

RESULTS

SFS Morphology

In the 20 cerebral hemispheres that were studied, we found the originating point of the SFS to lie anterior, posterior, or coincident to the precentral sulcus in 2, 14, and 4 specimens, respectively, and its end point was close to the frontal pole in all specimens (Figure 2). The sulcus was always parallel or almost parallel to the interhemispheric fissure and showed a continuous or interrupted pattern in 12 and 8

Figure 5. (*Left*) Meticulous dissection of the superior longitudinal fasciculus (SLF) fibers shows a white matter tract, radiating from the posterior part of the superior frontal gyrus to the frontal operculum, known as the frontal aslant tract (FAT). FAT is the second white mater layer en route to the lateral ventricle and its fibers lie just under the superior longitudinal fasciculus, as seen in the photo. Note that the anterior insular cortex has also been peeled, thus exposing the fibers of the extreme capsule, so as to facilitate differentiation of the white matter layers during the following dissection steps. (*Right*) A zoomed photo focusing on the fibers of the FAT. CS, central sulcus; EC, extreme capsule; FP, frontoparietal operculum; IN, insula; PCS, postcentral sulcus; PrCS, precentral sulcus; SFS, superior frontal sulcus.

specimens, respectively (Figure 2). In the hemispheres in which the sulcus was noncontinuous, it was divided by gyral bridges into 2 or 3 segments in 6 and 2 specimens, respectively. Opening the arachnoid and splitting the sulcus showed an internal configuration of 6 (on average) intrasulcal gyri (range, 3–9). The average sulcal length was 6.7 cm (range, 6–8.5) and its depth was 1.7 cm (range, 1.5–2.2). When the sulcus was noncontinuous (branching into either 2 or 3 parts), the length of the smaller sulcal segment ranged from 2.3 to 2.5 cm and that of the larger one from 3.5 to 4.5 cm. The distance between the SFS and the interhemispheric fissure varied between 2.1 and 3 cm, with an average value of 2.5 cm.

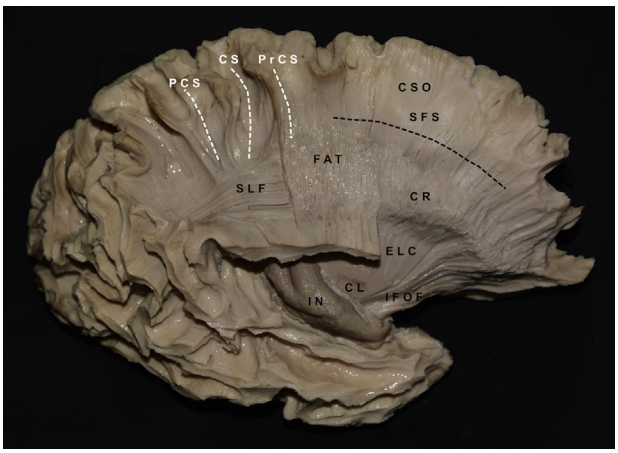

Figure 6. After the dissection of the extreme capsule at the level of the anterior insula (IN) and central core, the fibers of the external capsule become apparent, radiating to the white matter of the frontal lobe to form what is known as the corona radiata (CR) (up to the level of the lateral ventricle) and centrum semiovale (CSO) (above the level of the ventricle). The fibers of the external capsule (ELC) comprise the third consecutive white matter layer interposed between the superior frontal sulcus (SFS) and the lateral ventricle. Note also, at this dissection step, the fibers of the occipitofrontal fasciculus and the gray matter of the claustrum (CL). CS, central sulcus; FAT, frontal aslant tract; IFOF, inferior fronto-occipital fasciculus; IN, insula; PCS, postcentral sulcus; PrCS, precentral sulcus; SLF, superior longitudinal fasciculus.

Because of the high variability seen with regard to the surface anatomy of the frontal lobe, the process of mapping SFS morphology necessitates the precise and meticulous identification of the sulcus. In this context, its differentiation from the middle frontal and medial frontal sulci (in the cases in which these sulci are prominent in the cerebral surface) is crucial. For this purpose, we have recorded the presence of these sulci and measured their respective distance from the interhemispheric fissure in all 20 hemispheres included. Hence, the middle frontal sulcus was evident in 9/20 hemispheres, the medial frontal in 3/20 specimens, and both sulci were observed in 1 hemisphere. Respective distances measured from the interhemispheric fissure varied between 3.7 and 4.4 cm for the middle and 1.2 and 1.5 cm for the medial frontal sulcus.

White Matter Anatomy

We applied the fiber microdissection technique both in a lateral to medial and in a medial to lateral direction to investigate the white matter pathways lying in or adjacent to the surgical corridor used during the superior frontal transsulcal transventricular approach. The fiber tracts were categorized into discrete consecutive layers for educational purposes.

More specifically, during the cerebral dissection, we showed 5 white matter layers en route to the lateral ventricle. The first white matter layer identified on removing the cortical gray

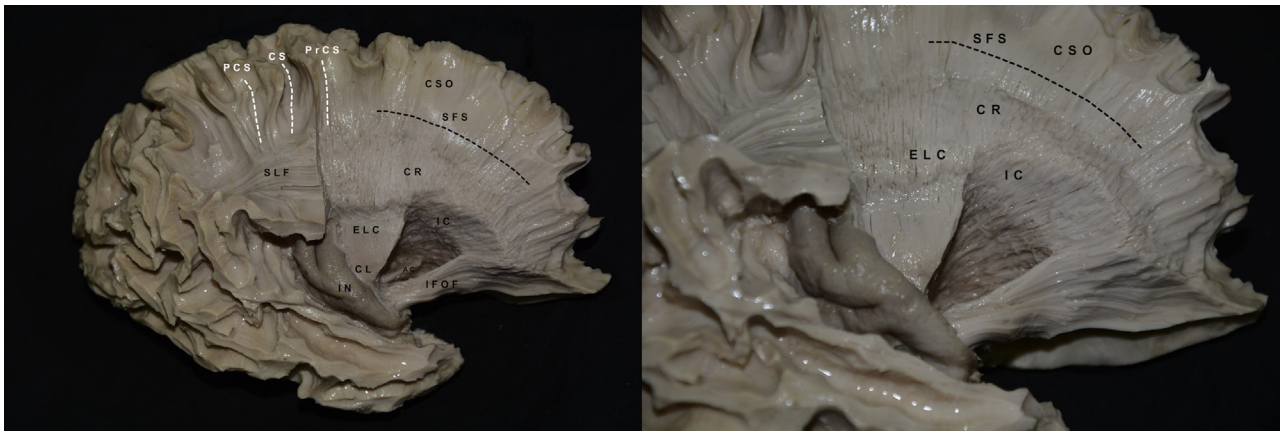

Figure 7. (*Left*) Gradual dissection of the external capsule (ELC) in its anterior part shows the fibers of the internal capsule (IC), which radiate to the hemisphere and form the fourth consecutive white matter layer en route to the lateral ventricle. (*Right*) A close-up delineates the difference in the fiber direction and trajectory of the external and internal capsules, respectively. Again, at the level of the superior frontal gyrus, these fiber bundles merge to form the centrum semiovale (CSO). AC, anterior commissure; CL, claustrum; CR, corona radiata; CS, central sulcus; IFOF, inferior fronto-occipital fasciculus; IN, insula; PCS, postcentral sulcus; PrCS, precentral sulcus; SFS, superior frontal sulcus; SLF, superior longitudinal fasciculus.

matter consists of the arcuate fibers, which connect anatomo-functionally adjacent cortical areas (i.e., the superior and middle frontal gyri) (Figure 3). Dissection of these fibers exposed the horizontally oriented fibers of the SLF, which were consistently found to run at the level of the middle frontal gyrus and therefore are not part of the white matter lying between the fundus of the SFS and the lateral ventricle (Figure 4). Meticulous dissection showed an oblique band of fibers radiating from the posterior part of the superior frontal gyrus to the level of the inferior frontal gyrus and particularly to the pars opercularis (Figure 5). This bundle is known as the frontal aslant tract (FAT) and comprises the second layer encountered when traversing the white matter lying between the posterior part of the SFS and the lateral ventricle.[28,29]

The subsequent white matter tracts interposed between the SFS and the lateral ventricle blend and form a dense and compact bundle broadly known as the corona radiata—centrum semiovale and therefore their proper discrimination is difficult, if not impossible. For this reason and to clarify the white matter architecture in this area, we had to extend the dissection to the

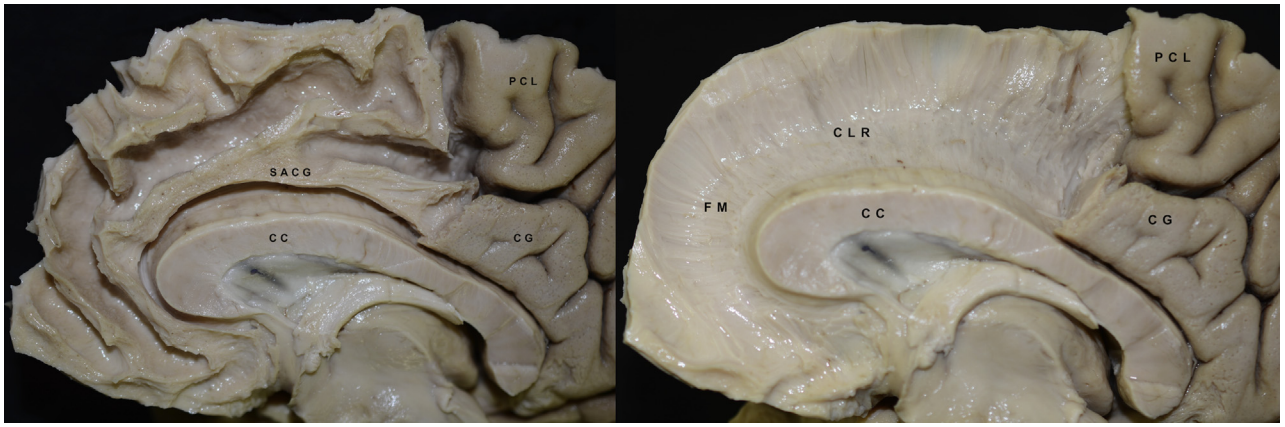

Figure 8. As mentioned in the text, to accurately expose the callosal radiations (CLR), the stepwise dissection should be directed from the medial to the lateral aspect of the hemisphere. In these photographs, the same hemisphere that underwent a lateral to medial dissection to show the fiber tracts up until the internal capsule is dissected from its medial aspect. (*Left*) The arcuate fibers of the medial frontal lobe and the superior arm of the cingulum (which are subsequently dissected to expose the CLR) are shown. (*Right*) The CLR comprise the fifth and last white matter layer before entering the lateral ventricle. CC, corpus callosum; CG, cingulate gyrus; FM, forceps minor; PCL, paracentral lobule; SACG, superior arm of the cingulum.

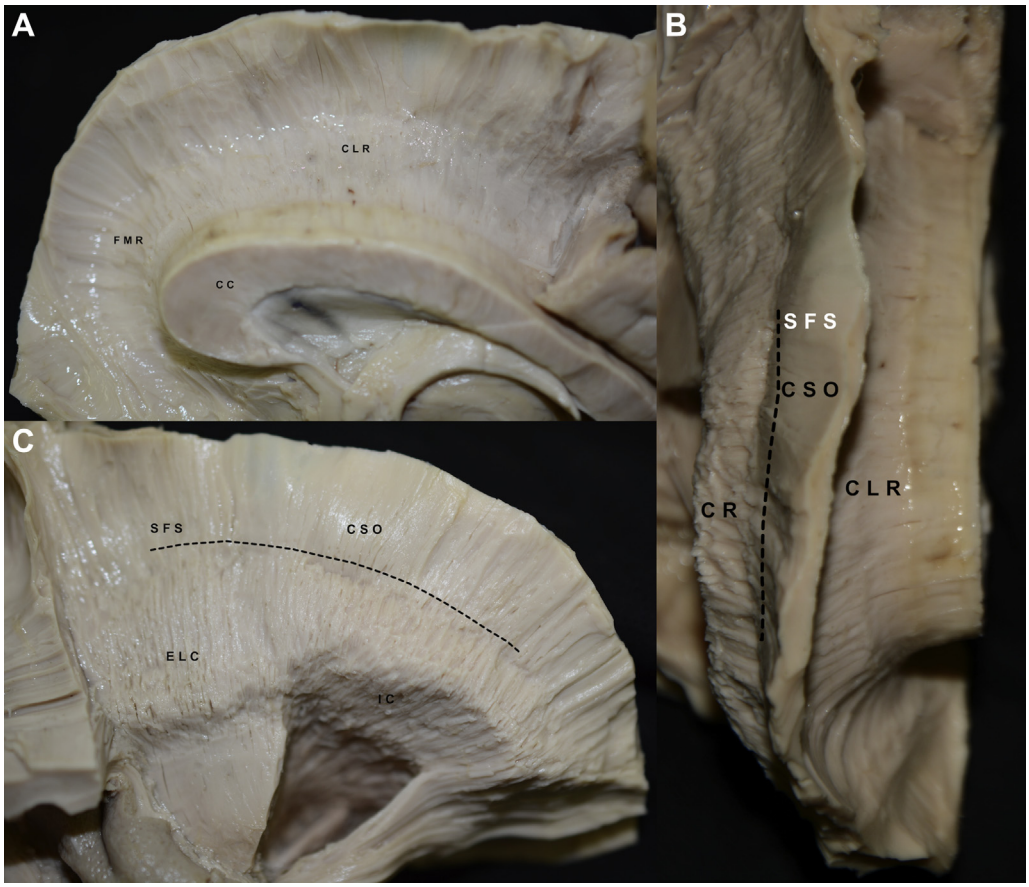

Figure 9. (**A**–**C**) Photographs of the same hemisphere, which has been dissected both in a lateromedial and mediolateral direction, during a 180° turn, showing the intermingling of the internal capsule (IC) and callosal radiations (CLR) to form the most medially placed part of the centrum semiovale (CSO). The level of the superior frontal sulcus (SFS) is also marked. CC, corpus callosum; CR, corona radiata; ELC, external capsule; FMR, forceps minor.

level of the insula and central core, in which the relevant fiber tracts become more obvious. Thus, progressive anatomic dissection at this level showed the fibers of the external capsule, radiating from the central core to the rest of the hemisphere and forming the third white matter layer en route to the ventricle (Figure 6). Removing the external capsule at the insular and central core level exposes the fibers of the anterior limb of the internal capsule, which blend with the external capsule at the periphery and form the corona radiata and centrum semiovale (Figure 7). The anterior limb of the internal capsule comprises the fourth consecutive white matter layer. A rough discrimination between the third and fourth white matter layers (i.e., external from internal capsule) is facilitated by the fact that the fibers of the internal capsule have a more oblique anteroposterior trajectory compared with those of the external capsule. Furthermore, by showing the gray matter of the putamen, we also expose the most lateral situated fibers of the internal capsule, because the external and internal capsules form the outer and inner envelope of this central core nucleus, respectively.

The fifth and last white matter layer traversed en route to the anterior ventricle is formed by the callosal radiations. These fibers show a dense consistency and intermingle with the fibers of the internal capsule in a nearly perpendicular angle, thus making their identification and illustration almost impossible when performing white matter dissections in a stepwise lateromedial direction. Therefore, to properly expose this white matter layer, the anatomic dissection is directed from the medial to the lateral aspect of the cerebral surface, as seen in Figure 8. The blending of the fibers of the corpus callosum and internal capsule to form the centrum semiovale is shown in Figure 9. During the last step of our dissection, we entered the lateral ventricle by incising the thin layer of the ependymal covering (Figure 10).

We have therefore shown that the white matter spanning the subcortical area between the SFS and the lateral ventricle consists of 5 consecutive and discrete layers of fibers that have to be

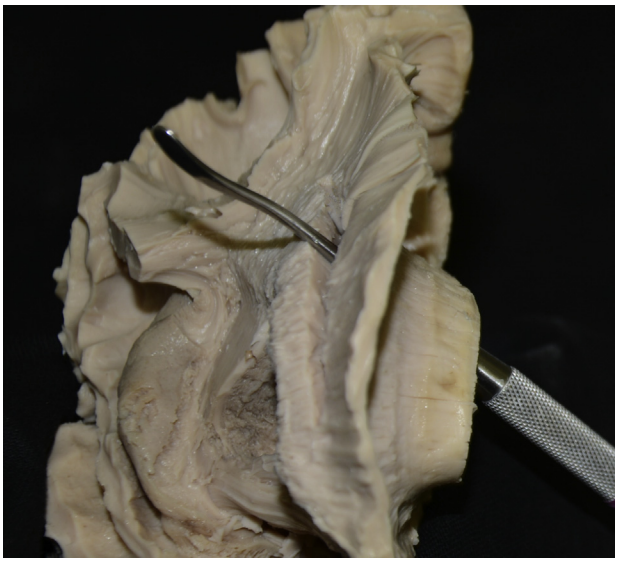

Figure 10. A photograph of the same specimen in a 90° turn, showing the access of the lateral ventricle through the centrum semiovale, at the level of the superior frontal sulcus.

traversed when performing the superior frontal transsulcal transventricular approach.

Coronal Cuts Along the Length of the SFS

The first cut, placed at the level of the SFS—precentral sulcus meeting point, showed this microneurosurgical key point to correspond to the body of the lateral ventricle in all specimens studied, and the average distance measured between the fundus of the sulcus and the ventricle was 1.3 cm (Figure 11). Regarding the second cut made at the level of the genu of the corpus callosum, and the third cut made in between the 2 previous cuts, the average respective distances measured between the sulcal fundus and the deep corresponding segments of the genu and the lateral ventricle were 2.1 and 1.5 cm (Figure 11).

The segment of the sulcus lying between the first and second cuts seemed to overly the lateral ventricle in all hemispheres studied and its average length was approximately 5 cm. The direction of the sulcus was always observed to point toward the lateral ventricle, thus offering natural anatomic orientation (Figure 11).

Cadaveric Approach

The superior frontal transsulcal approach to the anterior part of the ventricle is shown on the right side of 2 cadaveric heads. Initially, the head is secured in a neutral position with a 3-point skull clamp. Preferably, the single pin is placed on the right side (side of the approach) and the 2-pin rocker arm on the contralateral temporoparietal area, in a way that the pins do not interfere with the skin incision. The neck is slightly extended and the head is elevated so as to facilitate venous drainage. A transverse skin incision is marked depending on the location of the coronal suture and the cranial projection of the SFS—precentral sulcus meeting point, which according to the literature is located approximately 1 cm posterior to the bregma and 3 cm off the midline (Figure 12).[16] The skin incision is taken down to the galea aponeurotica (epicranium) and the underlying pericranium is harvested in a square fashion as a free graft, for closure purposes (Figure 13). The sagittal and coronal sutures are identified, burr holes are drilled, and a parasagittal craniotomy is then performed (Figure 14). The craniotomy should be approximately 6 × 6 cm, slightly cross the midline, and extend 1 cm posterior to the coronal suture, to expose an adequate part of the SFS for its microsurgical dissection (Figure 14). Underlying dura is freed from the bone and subsequently opened in a semicircular fashion with its base on the superior sagittal sinus. Bridging veins, when encountered, should be ideally dissected off their arachnoid mantle and mobilized so as to provide sufficient working space for the surgeon. Particularly, veins that are located posterior to the level of the coronal suture must be always preserved because of their tendency to cause serious venous infarction. On exposure of the cerebral surface, the SFS is identified and microsurgically opened from its arachnoid covering along its available length, which comes to an average of 4–5 cm (Figure 15). Dissection is taken down to the fundus of the sulcus, respecting the pial planes and preserving the arteries inside the sulcus. Once the sulcal fundus has been reached, wet cottonoids are placed over the exposed intrasulcal surfaces followed by self-retaining brain spatulas (Figure 15). As mentioned earlier, the trajectory of the sulcus and consequently of the brain retractors placed points toward the lateral ventricle, and hence, offers natural anatomic orientation for the subcortical dissection. A parenchymal transgression of approximately 2 cm leads directly to the right lateral ventricle.

DTI Tractography

Using the single ROI approach, the following white matter tracts were identified: short association frontal fibers (U-shaped fibers), FAT, external capsule, and thalamocortical and corticopontine projection fibers, which constitute the anterior limb of the internal capsule, and callosal fibers (Figure 16). In addition, tractography reconstruction identified the 3 subcomponents of SLF as well as the arcuate fasciculus (Figure 17). At the coronal plane, it was evident that the SLF I was the most proximal subcomponent, although it was not included in the brain area investigated. The SLF II, III and the arcuate fasciculus were traced in the white matter of the frontal operculum and the circular sulcus of the insula, distal to the aforementioned region. The previous tracts were identified bilaterally in both healthy volunteers.

DISCUSSION

The Superior Frontal Transsulcal Approach to the Anterior Ventricle: Anatomic and Functional Considerations

Normal brain violation is inevitable when dealing with intraventricular or periventricular lesions.[4,5] Thus, several surgical approaches have been proposed aiming to minimize parenchymal transgression, preserve eloquent cortical and subcortical anatomy, and optimize the applied operative trajectory. In this context, the concept of using cerebral fissures and sulci as

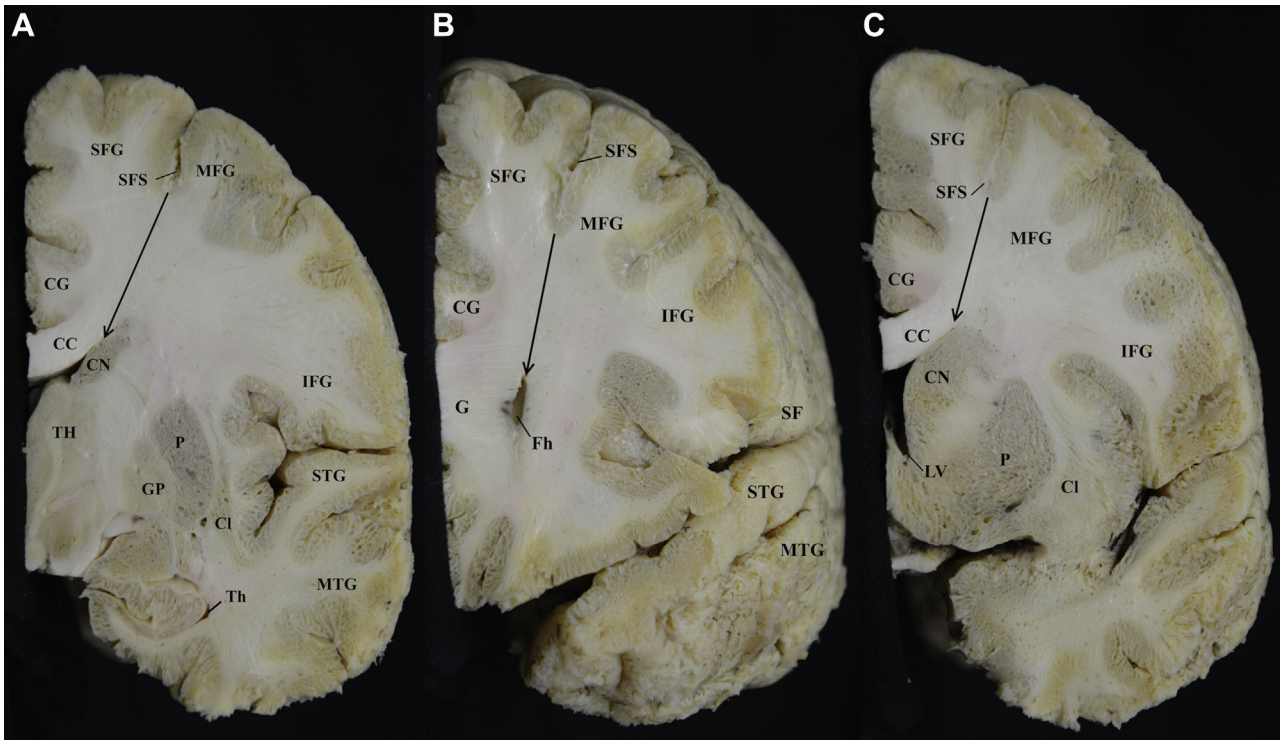

Figure 11. (**A**) Coronal cut at the level of the intersection point of the precentral with the superior frontal sulcus (SFS). The *black arrow* corresponds to the trajectory of the sulcus, which points toward the body of the lateral ventricle. (**B**) Coronal cut at the level of the genu of the corpus callosum (G). The trajectory of the sulcus (*black arrow*) points toward the frontal horn (Fh). (**C**) Coronal cut made in the middle of the distance between the first and second cuts. The trajectory of the sulcus (*black arrow*) is pointing toward the body of the lateral ventricle. CC, corpus callosum; CG, cingulate gyrus; CN, caudate nucleus; Cl, claustrum; GP, globus pallidus; IFG, inferior frontal gyrus; LV, lateral ventricle; MFG, middle frontal gyrus; MTG, middle temporal gyrus; P, putamen; SF, sylvian fissure; SFG, superior frontal gyrus; STG, superior temporal gyrus; TH, thalamus; Th, temporal horn.

surgical corridors to the ventricles has been proposed, because brain manipulation and retraction are (at least theoretically) reduced compared with the relevant transcortical routes. Hence, lesions located in the frontal horn, foramen of Monro, and anterior part of the body of the lateral ventricle can be safely and effectively accessed not only by opening the interhemispheric fissure and incising the anterior corpus callosum during the anterior transcallosal approach but also through the SFS by performing the superior frontal transsulcal transventricular approach.[16,22]

As mentioned in the previous section, after a tailored frontoparietal craniotomy and dural opening, the SFS is identified and dissected open from its arachnoid covering. Microsurgical splitting of the sulcus (for at least 3 cm along its length) allows for adequate intraoperative maneuverability and reduces excessive brain retraction, and arteries residing within the sulcus can be preserved by respecting the pial planes. Progressive dissection leads to the sulcal fundus and a subsequent subcortical transgression of approximately 1.5–2 cm leads to the anterior part of the ipsilateral ventricle. Image-guided stereotaxy and/or intraoperative ultrasonography can be also used to enhance safety and improve surgical precision. Veins draining into the superior sagittal sinus should ideally be preserved.

Although the approach appears to be straightforward, no detailed description of the SFS morphology and of the subcortical anatomy lying in or adjacent to the applied surgical corridor exists in the literature. Furthermore, most neurosurgeons have a limited understanding of the cortical and subcortical architecture of the lateral frontal lobe, mainly derived from standard neuroanatomic texts,[30-33] which could be characterized as oversimplistic in the modern era of surgical excellence and complication avoidance in operative neurosurgery. Therefore, to enhance neuroanatomic knowledge and inform surgical practice, we sought to investigate the sulcal and fiber tract anatomy involved during the superior frontal transsulcal transventricular approach to the anterior ventricular system.

More specifically, regarding SFS morphology, we observed that the sulcus was interrupted, branching in either 2 or 3 parts, in 40% of the specimens studied. This finding contradicts the traditional knowledge that the SFS is a continuous sulcus and raises concern about the optimal size and location of the craniotomy, because an uninterrupted sulcal segment of at least 3 cm is essential to perform the approach successfully.

Figure 12. A transverse skin incision is marked approximately 13 cm from the nasion, where the bregma and coronal suture are located according to the craniometric key points. The *blue dot* corresponds to the superior frontal—precentral sulcus meeting point, which is located averagely 1 cm posterior to the coronal suture and 3 cm off the midline.

Furthermore, a prominent medial and/or middle frontal sulcus may add perplexity to the precise identification of the SFS. In the 20 hemispheres studied, 12 (60%) showed 1 of the 2 aforementioned sulci whereas in 1 specimen (5%), both were observed, documenting that the surface anatomy of the frontal convexity can be highly variable and can potentially disorient the surgeon in the proper localization of the SFS. We noticed that within a maximum distance of 3 cm from the interhemispheric fissure, the SFS was either the only or the second, in a sequential order, sulcus (in the cases in which a medial frontal sulcus is prominent) from the midline. For these reasons, a detailed mapping of the SFS topography and configuration on the preoperative MRI scans along with the efficient use of intraoperative neuronavigation are crucial not only for tailoring the craniotomy to the patient's individual anatomy but also for deciding about the feasibility of the approach in a given clinical scenario (**Figure 18**).

In addition, we explored the subcortical architecture lying in or adjacent to the surgical trajectory applied during the approach through cadaveric white matter dissections and DTI studies in normal individuals. More specifically, the fiber microanatomic technique showed 5 discrete white matter layers en route to the anterior ventricular system (i.e., the arcuate fibers, the fibers of the FAT, the external capsule, the anterior limb of the internal capsule, and the anterior callosal radiations arising from the body and genu of the corpus callosum). The SLF is not traversed during the transsulcal transventricular approach, because it runs slightly inferior at the level of the middle frontal gyrus. Reassuringly, the tractographic study showed similar results to the cadaveric dissections. Arcuate fibers, FAT, fibers of the external capsule, the anterior limb of the internal capsule, and callosal fibers were identified as discrete subcomponents of this confined white matter area. Keeping with the cadaveric study, there was no evidence of SLF fibers running through the area of interest on DTI.

From a functional standpoint, most of the aforementioned white matter bundles have a rather obscure role and were traditionally considered as noneloquent in terms of their neurosurgical significance. Nonetheless, recent evidence deriving from studies on patients with progressive primary aphasia[29] and stuttering[34,35] has shown that the FAT, which connects the lateral prefrontal

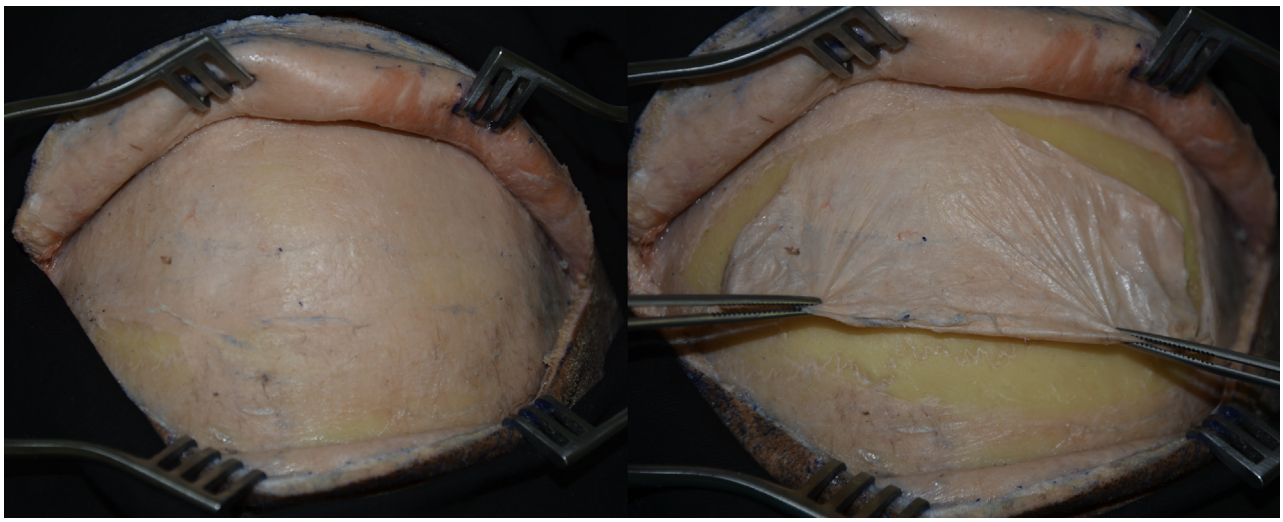

Figure 13. (*Left*) Skin incision is opened down to the pericranium and self-retaining retractors are placed. (*Right*) A layer of pericranium can be harvested for closure purposes.

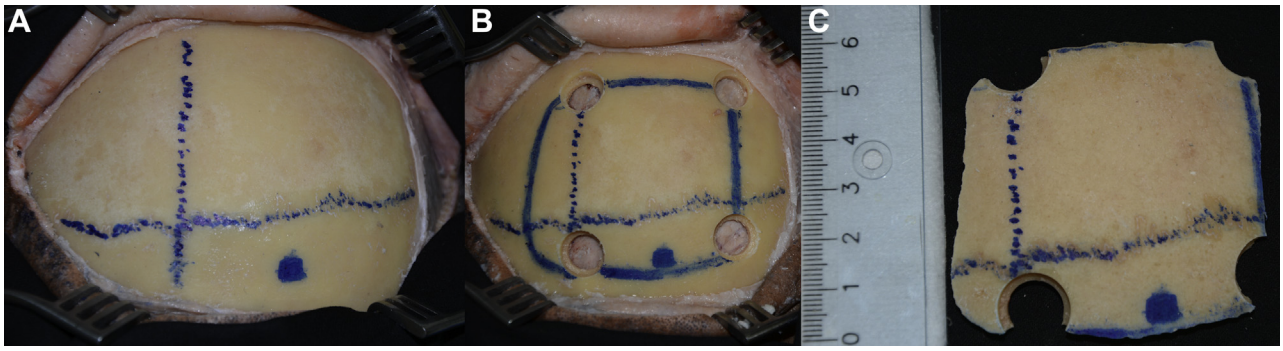

Figure 14. (**A**) Coronal suture, midline, and the superior frontal—recentral sulcus meeting point are marked with *blue* ink. (**B**) Burr holes are drilled and a 6-cm × 6-cm craniotomy, crossing both the coronal suture and the midline for approximately 1 cm, is marked. (**C**) A 6 × 6 cm bone flap is carefully elevated.

and medial premotor cortex to the pars triangularis,[28,36-41] participates in the complex pathway of verbal fluency and speech initiation.[29,34,42,43] Moreover, case studies of patients with diffuse low-grade gliomas[34,42] indicate that injury of this tract during surgery on the dominant hemisphere can result in transcortical motor aphasia,[36,44] a type of nonfluent aphasia with preserved repetition. Although its function on the nondominant hemisphere is largely unknown, recent case reports have suggested its implication on the anatomofunctional basis of the rare Foix-Chavany-Marie syndrome, which is mainly caused by bilateral opercular damage and consists of partial facioglossopharyngomasticatory paralysis.[45-49] In addition, the anterior limb of the internal capsule (the fourth consecutive white matter layer) is related to what is largely known in neuropsychology as set shifting ability. Set shifting is the ability to change focus between different environmental stimuli and is regarded as a reflection of cognitive flexibility.[50-53] Injury of this tract is associated with subtle attention deficits, which may be noticeable during meticulous neuropsychological assessments.

Coronal cuts showed that the trajectory of the SFS always points toward the lateral ventricle. Therefore, by keeping the direction of the subcortical dissection along the plane of the sulcus, the surgeon always encounters the lateral ventricle. This finding is consistent with previous anatomic studies[16,22-24] and confirms that the sulcus provides natural orientation for surgical practice. Moreover, the optimal area for intraoperative dissection proved to be the segment of the sulcus that extends approximately 5 cm anteriorly to the SFS—precentral sulcus meeting point, because it was shown to overlie the anterior part of the ipsilateral ventricle in all studied specimens. Nevertheless, surgical manipulations close to the SFS—precentral sulcus intersection point should ideally be avoided because of its inherent relationship to the motor strip (precentral sulcus)[54,55] premotor[56-60] and frontal visual eye fields.[61-64]

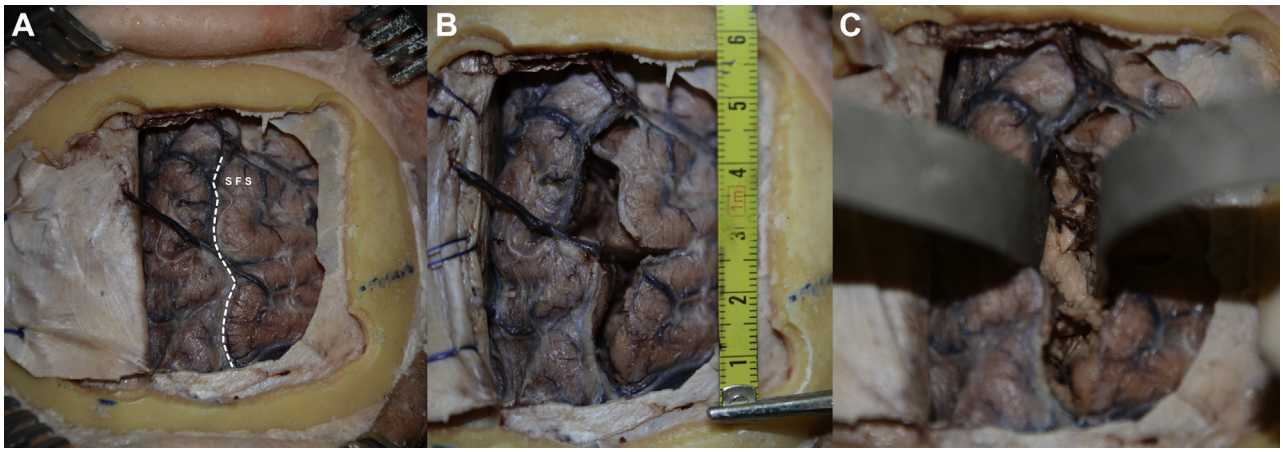

Figure 15. (**A**) The dura is opened with special attention paid to the bridging veins that drain to the superior sagittal sinus. The superior frontal sulcus (SFS) is identified and microsurgically freed from its arachnoid covering (**B**). The craniotomy fashioned allows for a microsurgical splitting of the superior frontal sulcus of approximately 5 cm, as shown in the photograph. (**C**) The trajectory of the brain spatulas placed equals that of the sulcus and, as mentioned, points toward the ipsilateral ventricle.

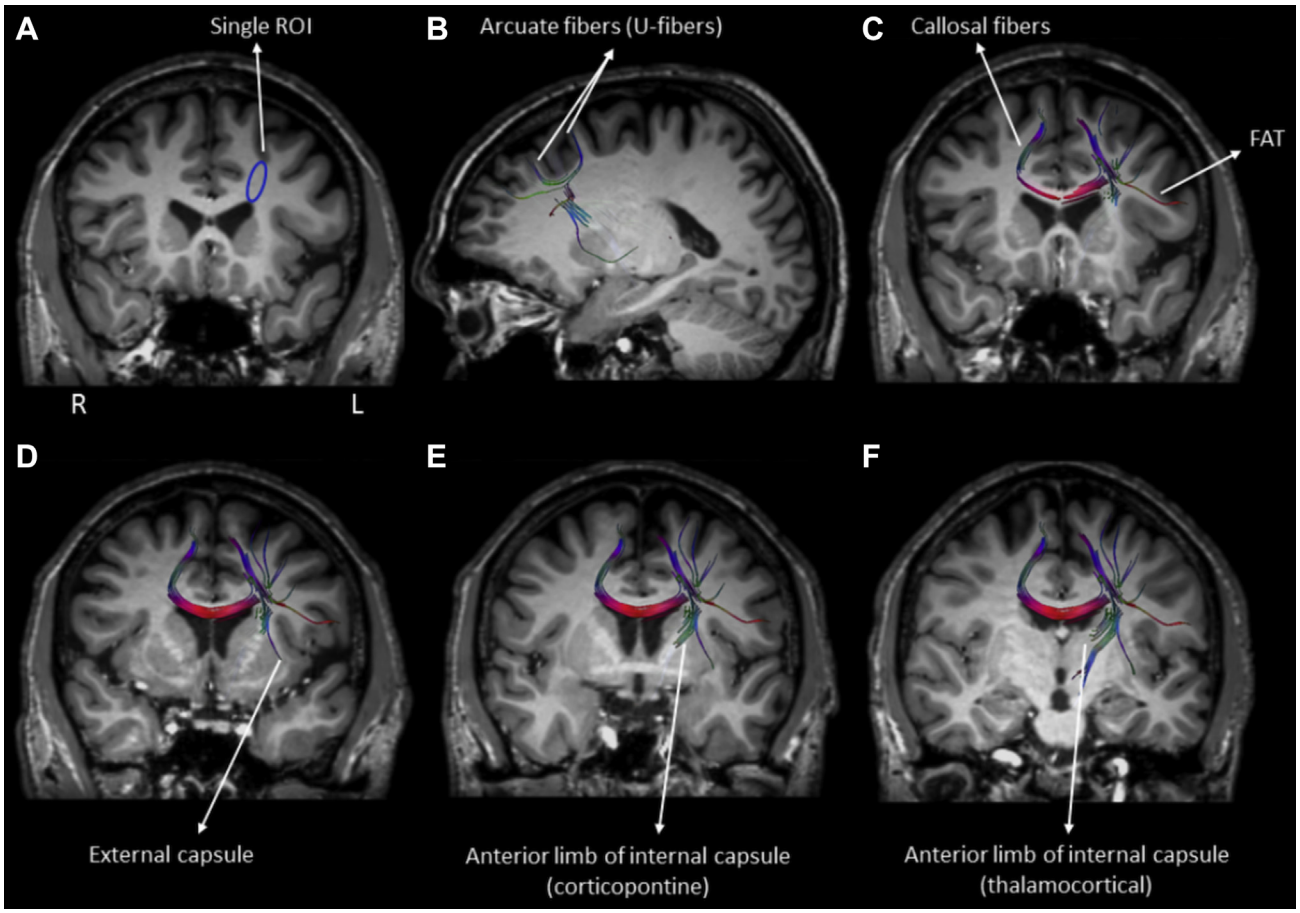

Figure 16. (**A**) The placement of the single region of interest (ROI) (at a coronal slice; left hemisphere [L]) including the white matter (WM) between the superior frontal sulcus and the anterior lateral ventricle, overlaid over a three-dimensional T1 image at the coronal plane. (**B**–**F**): Reconstruction of the white matter passing through the single ROI. The short U-shaped frontal arcuate fibers (**B**), the callosal fibers and the frontal aslant tract (FAT) (**C**), the fibers of the external capsule (**D**), and the anterior limb of the internal capsule (corticopontine projections [**E**] and thalamocortical projections [**F**]) overlaid over a three-dimensional T1 image at the coronal plane. The tracts are presented according to the RGB map with red, green and blue being assigned to right-left, anterior-posterior, and superior-inferior orientations. For visualization purposes, the projected tracts are overlaid over different slices compared with the one where the single ROI was placed. R, right hemisphere.

Given these considerations, when the configuration and morphology of the SFS, documented through meticulous preoperative assessment of the MRI scans (Figure 18), allows for the transsulcal approach to be safely carried out, the surgeon can fashion a 6-cm × 6-cm tailored parasagittal craniotomy, extending 1 cm posterior to the coronal suture and slightly crossing the midline (see the Results section), to adequately expose the superolateral frontal cerebral surface. Particular attention should be paid to the possible existence of a medial and/or middle frontal sulcus, which can disorient the surgeon, as well as to the regional venous anatomy.

Clinical Applicability and Limitations of the Superior Frontal Transsulcal Tranventricular Approach

The superior frontal transsulcal transventricular approach aims to minimize cortical and subcortical disruption and provide a relevant short working corridor and a straight surgical angle to the anterior part of the lateral ventricle and foramen of Monro. The operative trajectory applied avoids injuring the SLF, which runs at the level of the middle frontal gyrus and is related to speech and spatial awareness on the dominant and nondominant hemisphere, respectively. Furthermore, sensitive brain areas such as the corpus callosum and cingulate gyrus that are manipulated during the anterior transcallosal approach[6,10,11,65,66] and are functionally linked to bimanual synchronization,[67-70] motor planning,[67] learning,[65] and verbal memory[7,51,65] (the former) and attention, motivation, and emotional response[71] (the latter) are avoided.

However, the clinical applicability of the superior frontal transsulcal transventricular approach relies on the surface anatomy of the sulcus, because a fairly straight and uninterrupted sulcal segment of, at least, 3 cm is necessary for surgical manipulation. This fact in combination with the high morphologic variability of the superolateral frontal lobe anatomy renders

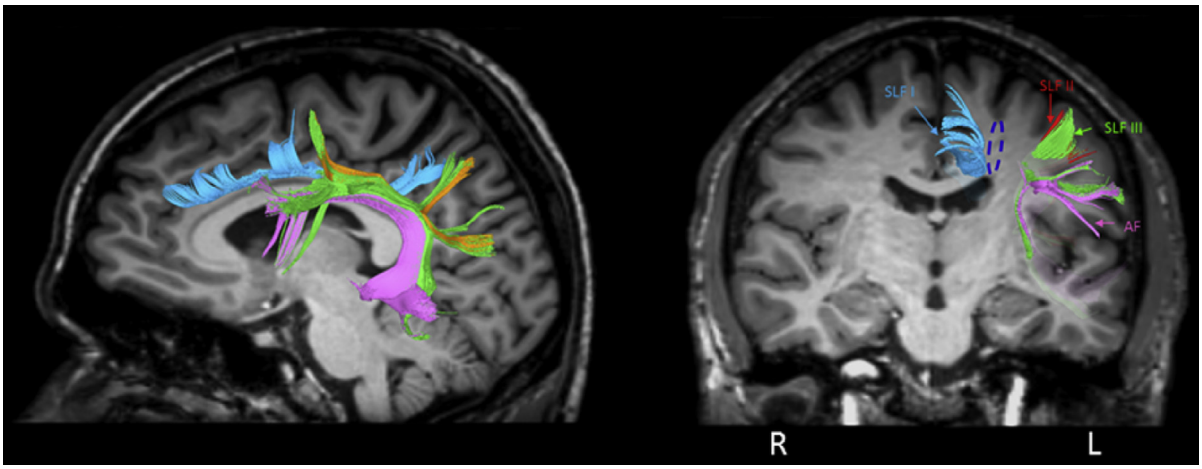

Figure 17. (*Left*) The reconstruction of the superior longitudinal fasciculus (SLF) I (*light blue*), SLF II (*orange*), SLF III (*green*), and arcuate fasciculus (AF) (*pink*) overlaid over a three-dimensional T1 midsagittal plane. (*Right*) Projection of the subcomponents of the left SLF (SLF I [*light blue*], SLF II [*red*], SLF III [*green*], and AF [*pink*]) overlaid over a three-dimensional T1 coronal plane and placement of the single region of interest (left hemisphere [L]) between the superior frontal sulcus and the anterior lateral ventricle. For visualization purposes, the single region of interest is overlaid over a different slice compared with the one originally placed. R, right hemisphere.

the decision of applying the approach in a given clinical scenario strongly dependent on the patient's unique cerebral anatomy. Hence, a potential contraindication to the transsulcal operative variant is the presence of a complex and noncontinuous SFS configuration, documented through preoperative imaging studies. In a recently reported study,[72] the investigators have managed to reduce the length of the sulcal dissection and further minimize brain transgression by using a small tubular retractor (internal diameter, 13.5 mm) during the transsulcal transventricular approach. After sulcal arachnoid dissection, the tubular retractor was inserted to the ventricles with the aid of frameless intraoperative navigation and, according to the study, allowed for a safe and effective intraventricular operative corridor.

Moreover, the risk of vascular injury to the very delicate cortical arteries living inside the sulcus, during its microsurgical arachnoid dissection, is greater than when performing a corticotomy at the top of a noneloquent gyrus and can result in postoperative infarction, thus increasing surgical morbidity. Nonetheless, a flawless microsurgical technique supplemented by a high microscope magnification and dynamic brain retraction can greatly reduce the possibility of this adverse event. Once the sulcus is

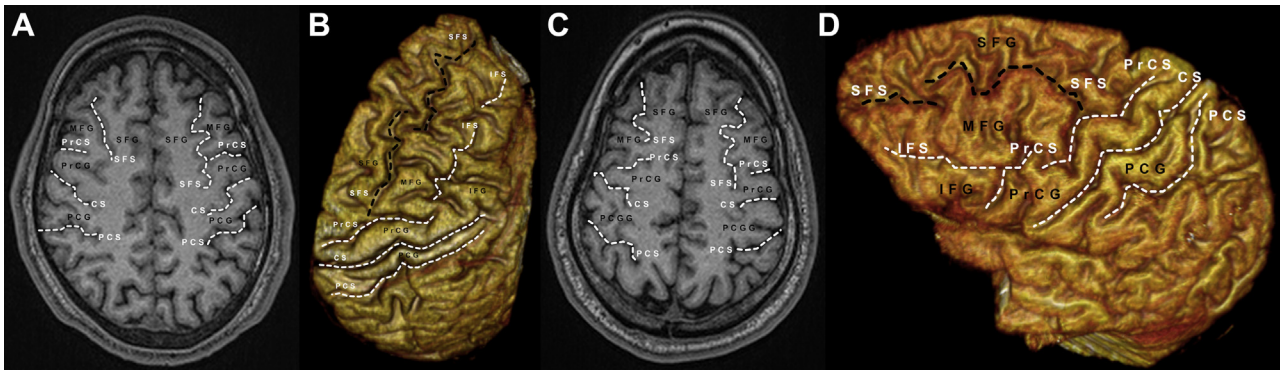

Figure 18. (**A**, **B**) Mapping of the superior frontal sulcus (SFS) morphology on preoperative magnetic resonance imaging scans. (**C**, **D**). Three-dimensional volume renderings of a right and left hemisphere, respectively, of the above magnetic resonance imaging scans. Note that in both cases, the superior frontal sulcus is interrupted and its originating point is coincident to the precentral sulcus (PrCS). Three-dimensional volume renderings are helpful because a detailed mapping of the sulcal topography and morphology can be obtained. CS, central sulcus; IFG, inferior frontal gyrus; IFS, inferior frontal sulcus; MFG, middle frontal gyrus; PCG, postcentral gyrus; PCS, postcentral sulcus; PrCG, precentral gyrus; SFG, superior frontal gyrus.

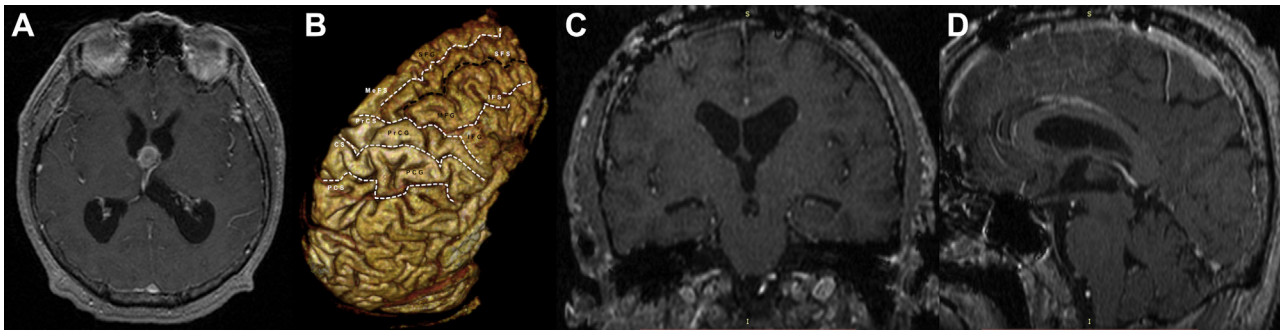

Figure 19. (**A**) An axial magnetic resonance imaging (MRI) scan showing a cystic lesion at the foramen of Monro and roof of anterior third ventricle, with maximum dimensions of 1.2 × 1.2 cm, most likely representing a colloid cyst. (**B**) Three-dimensional volume rendering of the above MRI scans showing a continuous superior frontal sulcus (SFS). (**C**, **D**) Coronal and sagittal cuts of the postoperative MRI scan of the patient showing the complete resection of the lesion. CS, central sulcus; IFG, inferior frontal gyrus; IFS, inferior frontal sulcus; MeFS, medial frontal sulcus; MFG, middle frontal gyrus; PCG, postcentral gyrus; PCS, postcentral sulcus; PrCG, precentral gyrus; PrCS, precentral sulcus; SFG, superior frontal gyrus.

dissected open, the presence of prominent intrasulcal gyri can convert the approach from a pure transsulcal to a transsulcal–transcortical approach during the surgeon's effort to reach the gray matter of the sulcal fundus, which has to be subsequently disrupted along the exposed sulcal length. Furthermore, without the presence of preoperative hydrocephalus, the relevant operative trajectory can risk injury to the head of the caudate nucleus and subcallosal stratum, thus increasing the risk of postoperative functional deficit.

Although the superior frontal transsulcal corridor to the lateral ventricle is less popular and more time consuming than its transcortical variant, it is nonetheless a very delicate approach, respecting the cortical anatomy and offering a wide operative trajectory particularly in the presence of dilated ventricles and for lesions located in the anterior part of the lateral ventricle and foramen of Monro. Meticulous preoperative planning, sound microneurosurgical skills, and thorough three-dimensional knowledge of both gray and white matter anatomy are mandatory for the safe and effective extrapolation of this approach to real operative settings.

Illustrative Case

A 52-year-old patient presented with a 3-month history of new-onset headaches and a broad-based gait and walking pattern. Clinical examination was otherwise normal and the neuropsychological assessment showed abnormal memory test results.

Imaging studies showed a cystic lesion located at the foramen of Monro and roof of the anterior third ventricle, with maximum dimensions of 1.2 × 1.2 cm, most likely presenting a colloid cyst of the region (Figure 19). Dilated ventricles were also noted on the preoperative scans.

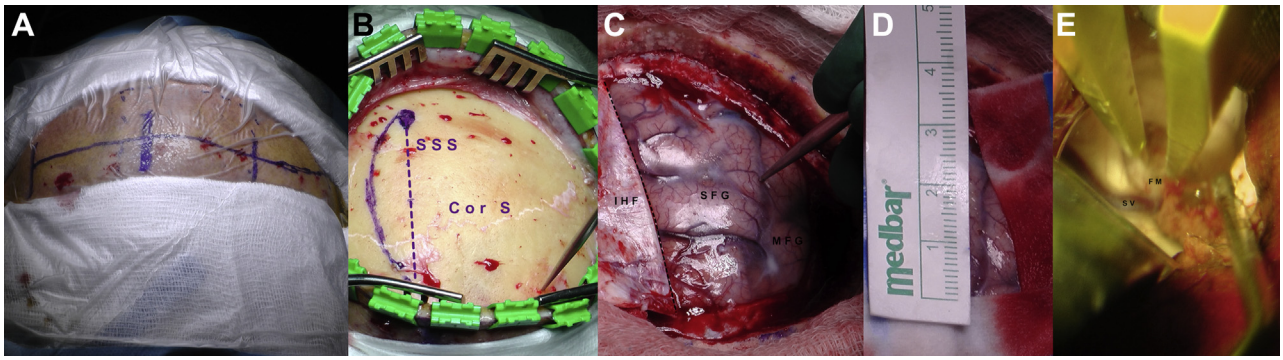

Figure 20. (**A**) Patient prepared and draped. A transverse skin incision is marked according to the craniometric points mentioned in the Results section. (**B**) Bony exposure after pericranial harvesting. The coronal suture (Cor S) is apparent. The midline is delineated and the limit of the craniotomy crossing to the opposite site is marked. The navigation tool points at the cranial projection of the superior frontal–precentral sulcus meeting point. (**C**) A 6-cm × 6-cm craniotomy is performed and the dura is elevated toward the superior sagittal sinus (SSS). The superior frontal sulcus (SFS) is identified and confirmed by intraoperative navigation. As already mentioned, the SFS is the only sulcus or the second in a sequential order within 3 cm from the interhemispheric fissure (IHF). (**D**) Wet cottonoids are placed over the cerebral surface for protection. A continuous, fairly straight segment of the SFS of approximately 3 cm is microsurgically dissected from its arachnoid covering to allow for the placement of self-retaining brain spatulas. (**E**) View of the direct trajectory and wide working corridor to the right lateral ventricle at the foramen of Monro (FM). The septal vein (SV) and the choroid plexus are also identified. MFG, middle frontal gyrus; SFG, superior frontal gyrus.

After informed consent, the patient underwent surgical exploration and resection of the cyst through a right superior frontal transsulcal transventricular approach with the use of intraoperative navigation. The cyst was successfully excised with no intraoperative issues and the patient's postoperative course was uneventful, leading to his discharge on the seventh day after surgery.

Meticulous preoperative planning regarding the SFS morphology is once again highlighted and shown (**Figure 19**). **Figure 20** shows some discrete steps of this approach.

CONCLUSIONS

Transsulcal approaches to access deep-seated cerebral lesions aim at minimizing normal brain violation and offering a shorter operative corridor.[22,72-78] To achieve this goal, a very detailed mapping of the relevant sulcal morphology on preoperative imaging along with a thorough understanding of the cerebral cortical and subcortical anatomy is mandatory so as to improve surgical precision and thus patient's outcome. In the context of the superior frontal transsulcal approach to the lateral ventricle, special emphasis should be placed on the highly variable anatomy of the superolateral frontal lobe along with the presence of preoperative hydrocephalus, factors that determine the feasibility of this approach in a given clinical case. If feasible, the superior transsulcal transventricular approach is a safe and effective operative variant in ventricular surgery, which definitely deserves more attention in modern neurosurgery.

ACKNOWLEDGMENTS

Author contributions to the study and manuscript preparation include the following: conception and design, C.K., F.L., A.V.K.; acquisition of data, A.V.K., C.K., F.L., F.C., S.K., G.P.S., E.L.; analysis and interpretation of data, C.K., A.V.K., F.L., G.P.S., F.C., E.K.; drafting the article, C.K., F.L., A.V.K.; critically revising the article, C.K., F.L., A.V.K., G.S.; reviewed submitted version of manuscript, all authors; administrative technical, material support; G.S.; study supervision, C.K., F.L., G.S.

REFERENCES

1. Nagata S, Rhoton AL Jr, Barry M. Microsurgical anatomy of the choroidal fissure. *Surg Neurol*. 1988; 30:3-59.
2. Ono M, Rhoton AL Jr, Peace D, Rodriguez RJ. Microsurgical anatomy of the deep venous system of the brain. *Neurosurgery*. 1984;15:621-657.
3. Rhoton AL Jr. The lateral and third ventricles. *Neurosurgery*. 2002;51:S207-S271.
4. Timurkaynak E, Rhoton AL Jr, Barry M. Microsurgical anatomy and operative approaches to the lateral ventricles. *Neurosurgery*. 1986;19: 685-723.
5. Yamamoto I, Rhoton AL Jr, Peace DA. Microsurgery of the third ventricle: Part I. Microsurgical anatomy. *Neurosurgery*. 1981;8:334-356.
6. Asgari S, Engelhorn T, Brondics A, Sandalcioglu IE, Stolke D. Transcortical or transcallosal approach to ventricle-associated lesions: a clinical study on the prognostic role of surgical approach. *Neurosurg Rev*. 2003;26: 192-197.
7. D'Angelo VA, Galarza M, Catapano D, Monte V, Bisceglia M, Carosi I. Lateral ventricle tumors: surgical strategies according to tumor origin and development—a series of 72 cases [Reprint in *Neurosurgery*. 2008;62(6 suppl 3):1066-1075; PMID: 18695527] *Neurosurgery*. 2005;56:36-45 [discussion: 36-45].
8. Desai KI, Nadkarni TD, Muzumdar DP, Goel AH. Surgical management of colloid cyst of the third ventricle—a study of 105 cases. *Surg Neurol*. 2002; 57:295-302 [discussion: 302-304].
9. Ellenbogen RG. Transcortical surgery for lateral ventricular tumors. *Neurosurg Focus*. 2001;10:E2.
10. Kasowski H, Piepmeier JM. Transcallosal approach for tumors of the lateral and third ventricles. *Neurosurg Focus*. 2001;10:E3.
11. Mazza M, Di Rienzo A, Costagliola C, Roncone R, Casacchia M, Ricci A, et al. The interhemispheric transcallosal-transversal approach to the lesions of the anterior and middle third ventricle: surgical validity and neuropsychological evaluation of the outcome. *Brain Cogn*. 2004;55:525-534.
12. Nayar VV, DeMonte F, Yoshor D, Blacklock JB, Sawaya R. Surgical approaches to meningiomas of the lateral ventricles. *Clin Neurol Neurosurg*. 2010; 112:400-405.
13. Park ES, Cho YH, Kim JH, Kim SJ, Khang SK, Kim CJ. Frontal transcortical approach in 12 central neurocytomas. *Acta Neurochir (Wien)*. 2012;154: 1961-1971 [discussion: 1972].
14. Shapiro S, Rodgers R, Shah M, Fulkerson D, Campbell RL. Interhemispheric transcallosal subchoroidal fornix-sparing craniotomy for total resection of colloid cysts of the third ventricle. *J Neurosurg*. 2009;110:112-115.
15. Pia HW. Microsurgery of gliomas. *Acta Neurochir (Wien)*. 1986;80:1-11.
16. Ribas GC, Yasuda A, Ribas EC, Nishikuni K, Rodrigues AJ Jr. Surgical anatomy of microneurosurgical sulcal key points. *Neurosurgery*. 2006; 59:ONS177-ONS210 [discussion: ONS210-ONS211].
17. Yasargil MG. A legacy of microneurosurgery: memoirs, lessons, and axioms. *Neurosurgery*. 1999; 45:1025-1092.
18. Yasargil MG. *Microneurosurgery*. Vol. 1. Stuttgart: Thieme; 1984.
19. Yasargil MG. *Microneurosurgery*. Vol. 4A. Stuttgart: Thieme; 1994.
20. Yasargil MG. *Microneurosurgery*. Vol. 4B. Stuttgart: Thieme; 1996.
21. Yasargil MG, Abdulrauf SI. Surgery of intraventricular tumors. *Neurosurgery*. 2008;62:1029-1040 [discussion: 1040-1041].
22. Harkey HL, al-Mefty O, Haines DE, Smith RR. The surgical anatomy of the cerebral sulci. *Neurosurgery*. 1989;24:651-654.
23. Ono M, Kubik S, Abernathey CD. *Atlas of the Cerebral Sulci*. Stuttgart: Thieme; 1990.
24. Ribas GC. The cerebral sulci and gyri. *Neurosurg Focus*. 2010;28:E2.
25. Klingler J, Ludwig E. *Atlas Cerebri Humani*. Basel/New York, NY: Karger; 1956.
26. Koutsarnakis C, Liakos F, Kalyvas AV, Sakas DE, Stranjalis G. A laboratory manual for stepwise cerebral white matter fiber dissection. *World Neurosurg*. 2015;84:483-493.
27. Kamali A, Flanders AE, Brody J, Hunter JV, Hasan KM. Tracing superior longitudinal fasciculus connectivity in the human brain using high resolution diffusion tensor tractography. *Brain Struct Funct*. 2014;219:269-281.
28. Catani M, Dell'acqua F, Vergani F, Malik F, Hodge H, Roy P, et al. Short frontal lobe connections of the human brain. *Cortex*. 2012;48: 273-291.
29. Catani M, Mesulam MM, Jakobsen E, Malik F, Martersteck A, Wieneke C, et al. A novel frontal pathway underlies verbal fluency in primary progressive aphasia. *Brain*. 2013;136: 2619-2628.
30. Nieuwenhuys R, Voogd J, Van Huijzen C. *The Human Central Nervous System: A Synopsis and Atlas*. Berlin: Springer-Verlag; 1988.
31. Parent A. *Carpenter's Human Neuroanatomy*. Baltimore, MD: Williams & Wilkins; 1996.
32. Rhoton AL. *Rhoton's Cranial Anatomy and Surgical Approaches*. Philadelphia, PA: Lippincott Williams & Wilkins; 2003.
33. Snell RS. *Clinical Neuroanatomy*. Baltimore, MD: Lippincott Williams & Wilkins; 2010.

34. Kemerdere R, de Champfleur NM, Deverdun J, Cochereau J, Moritz-Gasser S, Herbet G, et al. Role of the left frontal aslant tract in stuttering: a brain stimulation and tractographic study. *J Neurol*. 2016;263:157-167.

35. Kronfeld-Duenias V, Amir O, Ezrati-Vinacour R, Civier O, Ben-Shachar M. The frontal aslant tract underlies speech fluency in persistent developmental stuttering. *Brain Struct Funct*. 2016;221:365-381.

36. Ford A, McGregor KM, Case K, Crosson B, White KD. Structural connectivity of Broca's area and medial frontal cortex. *Neuroimage*. 2010;52:1230-1237.

37. Fujii M, Maesawa S, Ishiai S, Iwami K, Futamura M, Saito K. Neural basis of language: an overview of an evolving model. *Neurol Med Chir (Tokyo)*. 2016;56:379-386.

38. Kinoshita M, Miyashita K, Tsutsui T, Furuta T, Nakada M. Critical neural networks in awake surgery for gliomas. *Neurol Med Chir (Tokyo)*. 2016;56:674-686.

39. Kinoshita M, Shinohara H, Hori O, Ozaki N, Ueda F, Nakada M, et al. Association fibers connecting the Broca center and the lateral superior frontal gyrus: a microsurgical and tractographic anatomy. *J Neurosurg*. 2012;116:323-330.

40. Lawes IN, Barrick TR, Murugam V, Spierings N, Evans DR, Song M, et al. Atlas-based segmentation of white matter tracts of the human brain using diffusion tensor tractography and comparison with classical dissection. *Neuroimage*. 2008;39:62-79.

41. Martino J, De Lucas EM. Subcortical anatomy of the lateral association fascicles of the brain: a review. *Clin Anat*. 2014;27:563-569.

42. Fujii M, Maesawa S, Motomura K, Futamura M, Hayashi Y, Koba I, et al. Intraoperative subcortical mapping of a language-associated deep frontal tract connecting the superior frontal gyrus to Broca's area in the dominant hemisphere of patients with glioma. *J Neurosurg*. 2015;122:1390-1396.

43. Kinoshita M, de Champfleur NM, Deverdun J, Moritz-Gasser S, Herbet G, Duffau H. Role of fronto-striatal tract and frontal aslant tract in movement and speech: an axonal mapping study. *Brain Struct Funct*. 2015;220:3399-3412.

44. Alexander MP, Benson DF, Stuss DT. Frontal lobes and language. *Brain Lang*. 1989;37:656-691.

45. Duffau H, Karachi C, Gatignol P, Capelle L. Transient Foix-Chavany-Marie syndrome after surgical resection of a right insulo-opercular low-grade glioma: case report. *Neurosurgery*. 2003;53:426-431 [discussion: 431].

46. Martino J, de Lucas EM, Ibanez-Plagaro FJ, Valle-Folgueral JM, Vazquez-Barquero A. Foix-Chavany-Marie syndrome caused by a disconnection between the right pars opercularis of the inferior frontal gyrus and the supplementary motor area. *J Neurosurg*. 2012;117:844-850.

47. Mateos V, Salas-Puig J, Campos DM, Carrero V, Andermann F. Acquired bilateral opercular lesions or Foix-Chavany-Marie syndrome and eating epilepsy. *J Neurol Neurosurg Psychiatry*. 1995;59:559-560.

48. Popescu M, Sandu AM, Onose G, Sinescu RD, Grigorean VT. Foix-Chavany-Marie syndrome caused by bilateral opercular lesions: right side tumor and left side ischemic stroke. *Rev Neurol*. 2013;57:333-335.

49. Theys T, Van Cauter S, Kho KH, Vijverman AC, Peeters RR, Sunaert S, et al. Neural correlates of recovery from Foix-Chavany-Marie syndrome. *J Neurol*. 2013;260:415-420.

50. Greenberg BD, Malone DA, Friehs GM, Rezai AR, Kubu CS, Malloy PF, et al. Three-year outcomes in deep brain stimulation for highly resistant obsessive-compulsive disorder. *Neuropsychopharmacology*. 2006;31:2384-2393.

51. Jeeves MA, Simpson DA, Geffen G. Functional consequences of the transcallosal removal of intraventricular tumours. *J Neurol Neurosurg Psychiatry*. 1979;42:134-142.

52. Koch K, Reess TJ, Rus OG, Zimmer C, Zaudig M. Diffusion tensor imaging (DTI) studies in patients with obsessive-compulsive disorder (OCD): a review. *J Psychiatr Res*. 2014;54:26-35.

53. Sullivan EV, Zahr NM, Rohlfing T, Pfefferbaum A. Fiber tracking functionally distinct components of the internal capsule. *Neuropsychologia*. 2010;48:4155-4163.

54. Boling W, Olivier A, Bittar RG, Reutens D. Localization of hand motor activation in Broca's pli de passage moyen. *J Neurosurg*. 1999;91:903-910.

55. Yousry TA, Schmid UD, Jassoy AG, Schmidt D, Eisner WE, Reulen HJ, et al. Topography of the cortical motor hand area: prospective study with functional MR imaging and direct motor mapping at surgery. *Radiology*. 1995;195:23-29.

56. Duffau H, Capelle L, Denvil D, Gatignol P, Sichez N, Lopes M, et al. The role of dominant premotor cortex in language: a study using intraoperative functional mapping in awake patients. *Neuroimage*. 2003;20:1903-1914.

57. Freund HJ. Functional organization of the human supplementary motor area and dorsolateral premotor cortex. *Adv Neurol*. 1996;70:263-269.

58. Freund HJ, Hummelsheim H. Lesions of premotor cortex in man. *Brain*. 1985;108:697-733.

59. Halsband U, Freund HJ. Premotor cortex and conditional motor learning in man. *Brain*. 1990;113:207-222.

60. van Geemen K, Herbet G, Moritz-Gasser S, Duffau H. Limited plastic potential of the left ventral premotor cortex in speech articulation: evidence from intraoperative awake mapping in glioma patients. *Hum Brain Mapp*. 2014;35:1587-1596.

61. Guitton D, Buchtel HA, Douglas RM. Frontal lobe lesions in man cause difficulties in suppressing reflexive glances and in generating goal-directed saccades. *Exp Brain Res*. 1985;58:455-472.

62. Henik A, Rafal R, Rhodes D. Endogenously generated and visually guided saccades after lesions of the human frontal eye fields. *J Cogn Neurosci*. 1994;6:400-411.

63. Pierrot-Deseilligny C, Rivaud S, Penet C, Rigolet MH. Latencies of visually guided saccades in unilateral hemispheric cerebral lesions. *Ann Neurol*. 1987;21:138-148.

64. Vernet M, Quentin R, Chanes L, Mitsumasu A, Valero-Cabre A. Frontal eye field, where art thou? Anatomy, function, and non-invasive manipulation of frontal regions involved in eye movements and associated cognitive operations. *Front Integr Neurosci*. 2014;8:66.

65. Peltier J, Roussel M, Gerard Y, Lassonde M, Deramond H, Le Gars D, et al. Functional consequences of a section of the anterior part of the body of the corpus callosum: evidence from an interhemispheric transcallosal approach. *J Neurol*. 2012;259:1860-1867.

66. Spina A, Gagliardi F, Bailo M, Boari N, Caputy AJ, Mortini P. Comparative anatomical study on operability in surgical approaches to the anterior part of the third ventricle. *World Neurosurg*. 2016;95:457-463.

67. Caille S, Sauerwein HC, Schiavetto A, Villemure JG, Lassonde M. Sensory and motor interhemispheric integration after section of different portions of the anterior corpus callosum in nonepileptic patients. *Neurosurgery*. 2005;57:50-59 [discussion: 50-59].

68. Eliassen JC, Baynes K, Gazzaniga MS. Anterior and posterior callosal contributions to simultaneous bimanual movements of the hands and fingers. *Brain*. 2000;123:2501-2511.

69. Jeeves MA, Silver PH, Jacobson I. Bimanual co-ordination in callosal agenesis and partial commissurotomy. *Neuropsychologia*. 1988;26:833-850.

70. Preilowski BF. Possible contribution of the anterior forebrain commissures to bilateral motor coordination. *Neuropsychologia*. 1972;10:267-277.

71. Devinsky O, Morrell MJ, Vogt BA. Contributions of anterior cingulate cortex to behaviour. *Brain*. 1995;118:279-306.

72. Eliyas JK, Glynn R, Kulwin CG, Rovin R, Young R, Alzate J, et al. Minimally invasive transsulcal resection of intraventricular and periventricular lesions through a tubular retractor system: multicentric experience and results. *World Neurosurg*. 2016;90:556-564.

73. Germano IM. Transsulcal approach to mesiotemporal lesions. Anatomy, technique, and report of three cases. *Neurosurg Focus*. 1996;1:e4.

74. Jabre A, Patel A. Transsulcal microsurgical approach for subcortical small brain lesions:

technical note. *Surg Neurol*. 2006;65:312-313 [discussion: 313-314].

75. Mikuni N, Hashimoto N. A minimally invasive transsulcal approach to the paracentral inner lesion. *Minim Invasive Neurosurg*. 2006;49:291-295.

76. Miyagi Y, Shima F, Ishido K, Araki T, Kamikaseda K. Inferior temporal sulcus as a site of corticotomy: magnetic resonance imaging analysis of individual sulcus patterns. *Neurosurgery*. 2001;49:1394-1397 [discussion: 1397-1398].

77. Nagata S, Sasaki T. Lateral transsulcal approach to asymptomatic trigonal meningiomas with correlative microsurgical anatomy: technical case report. *Neurosurgery*. 2005;56:E438 [discussion: E438].

78. Zhou H, Miller D, Schulte DM, Benes L, Rosenow F, Bertalanffy H, et al. Transsulcal approach supported by navigation-guided neurophysiological monitoring for resection of paracentral cavernomas. *Clin Neurol Neurosurg*. 2009;111:69-78.

Conflict of interest statement: The authors declare that the article content was composed in the absence of any commercial or financial relationships that could be construed as a potential conflict of interest.

Received 22 December 2016; accepted 28 June 2017

Citation: World Neurosurg. (2017) 106:339-354.
http://dx.doi.org/10.1016/j.wneu.2017.06.161

*Journal homepage: **www.WORLDNEUROSURGERY.org***

*Available online: **www.sciencedirect.com***